Born-approximation electron ionization cross sections for Al^{n+} $(0 \leq n \leq 11)$ and some ions of the Na isoelectronic sequence

E. J. McGuire
Sandia National Laboratories, Albuquerque, New Mexico 87185
(Received 2 February 1982)

Generalized oscillator strengths (GOS) for excitation and ionization of all occupied shells of Al^{n+} $(0 \leq n \leq 11)$, and the Mg, Si, Ni, and Zn ions of the sodium isoelectronic sequence were calculated. The Al-ion GOS were used elsewhere to compute proton stopping power. There were no measurements or other calculations on stopping power with which to compare our calculations. Here the Al-ion GOS are used to calculate electron-ion ionization cross sections, including the effects of excitation followed by autoionization. The cross sections agree to 20% or better with measurements and other calculations, except near threshold. Calculations are also performed for five ions of the Na isoelectronic sequence to examine the relative importance of direct ionization versus excitation followed by autoionization. Comparison with recent measurements on three of these ions (Mg^{1+}, Al^{2+}, and Si^{3+}) shows agreement to better than 10% in some cases, and no worse than 20% in any case.

I. INTRODUCTION

The stopping power for protons in aluminum is of interest to the light-ion-beam fusion program. Recently[1] we calculated the stopping power of Al ions both by using Bethe[2] theory (calculating I, the Bethe mean excitation energy, for all the ions from complete sets of photoabsorption cross sections), and by explicitly calculating the contribution to the stopping power of excitation and ionization of each occupied subshell. The explicit calculations were done using the generalized oscillator strength (GOS) formulation of the Born approximation.[3] The same GOS can be used to calculate electron-ion excitation and ionization cross sections in Al ions. Far more information is available for electron-ion inelastic collisions than for proton-ion collisions. Comparison of electron ionization cross sections calculated with our GOS with experiment and other, more sophisticated, calculations serves to validate our GOS data base. Because of the computational complexity of the more sophisticated calculations, they are limited in the range of incident electron energy covered. Because of their relative computational simplicity, Born-approximation calculations are not so limited. Our aim is to tie the stopping-power calculations into the general body of inelastic scattering physics. Earlier[3] we generated sets of GOS for ions of C, N, O, and F which are possible alternatives to protons in the light-ion fusion program. While our ultimate aim is to study in detail the stopping power of these ions in high-Z targets, to validate the GOS for these ions, we used the GOS to calculate electron ionization cross sections to compare with both experiment and other calculations.

For Al ions there are few experimental data available, i.e., measurements on neutral[4] and sodiumlike Al.[5] In both instances inner-shell excitation followed by autoionization plays a significant role. In addition to Al^{2+}, Crandall *et al.*[5] have measured electron ionization cross sections in Mg^{1+} and Si^{3+}. To examine the role of excitation followed by autoionization, GOS calculations were done for MG^{1+}, Si^{3+}, Ni^{17+}, and Zn^{19+}. The nickel and zinc ions lie between Fe^{15+} and Mo^{31+} studied by Cowan and Mann.[6]

In Sec. II the treatment of autoionization is discussed. Since the principal subjects of these calculations are excitation and ionization, the treatment of autoionization is simplified. In Sec. III, the Al-ion calculations are presented and discussed; in Sec. IV the sodium isoelectronic sequence results are presented and discussed and conclusions stated in Sec. V.

II. AUTOIONIZATION

The machinery of the GOS calculations is discussed in Ref. 3 and earlier papers. In treating autoionization following excitation, the procedure used was different from that used in Ref. 3. There, for C, N, and O ions, many of the levels of the ex-

cited configuration $1s^2 2s\,^1 2p^m nl$ could be found in Moore's tables.[7] For the Al ions and those of the Na isoelectronic sequence there are few spectroscopic assignments just below and above the ionization threshold. However, the relevant terms of $1s^2 2s\,^1 2p^m$ in the next higher ionization stage were generally available in Moore's tables.[7] These, coupled with the calculated one-electron ionization energy for the nl orbital allowed me to make a fairly accurate determination of whether the $1s^2 2s\,^1 2p^m nl$ levels were bound. If the terms were not bound, I assume they autoionized with unity autoionization yield.

Table I illustrates the procedure for Al^{5+}. The ionization threshold is at 1 536 300 cm^{-1}. The Al^{6+} $2s\,^1 2p^3\,^4P$ and ^2P levels are at 1 818 300 and 2 012 300 cm^{-1}, respectively. The estimated $2s\,^1 2p^3\,^4P(nl)$ and $2s\,^1 2p^3\,^2P(nl)$ level energies are listed. For the $2s\,^1 2p^3\,^4P 3s\,^3P$ level the estimated level energy is 10 000 cm^{-1} less than the measured value. It was assumed that the energy difference would decrease as one goes to higher-lying levels, and that for $nl = 3s$, $3p$, $3d$, $4s$, and $4p$ the $2s\,^1 2p^3\,^4P(nl)$ terms are bound, while for $nl = 4d$, $5s$, $5p$, and $5d$ the levels autoionize. These ten levels are the one-electron excited levels included in the calculation. For the $2s\,^1 2p^3\,^2P(nl)$ levels it was assumed that only the $nl = 3s$ and $3p$ levels were bound. Table I indicates that for the $2s\,^1 2p^3\,^2P(3s)$ level, our estimate is 30 000 cm^{-1} higher than the observed level energy. If a difference comparable to this also exists for the $2s\,^1 2p^3\,^2(3d)$ level then it would be bound, rather than autoionizing. This would change the excitation-autoionization contribution to the total ionization cross section by amounts ranging from 50% at 200 eV to 25% at 10 keV. However, the autoionization-excitation contribution to the total ionization cross section ranges from 20% near 200 eV to less than 10% at 10 keV. That is, assignment of the $2s\,^1 2p^3\,^2P(3d)$ level as autoionizing will change the total cross section by less than 10%.

In Ref. 3, I discussed the excited $2s\,^1 2p\,^1[^3P,^1P]nl\,^2L$ terms in the boron isoelectronic sequence, pointing out that for $L = l \pm 1$, one expects autoionization if energetically allowed. However, for $L = l$, conservation of parity, spin, and angular momentum forbids autoionzation in LS coupling. For boronlike Al, these considerations were irrelevant as none of the excited levels included in the calculation had energy above the ionization threshold. However, for neutral Al and the sodium isoelectronic sequence, the argument should apply. That is, in the excitation event

$$3s^2 3p\,^1 2P + e \rightarrow 3s\,^1 3p\,^1[^1P,^3P](nl)(^2l+1,^2l,^2l-1) + e$$

for neutral Al, and

$$2p^6 3s^2 S + e \rightarrow 2p^5 3s\,^1[^1P,^3P](nl)(^2l+1,^2l,^2l-1) + e$$

for the Na isoelectronic sequence, the autoionization matrix element involves initial $3p$ and nl electrons and final $3s$ and ϵl_c electrons for neutral Al (initial $3s$ and nl electrons and final $2p$ and ϵl_c electrons for the Na isoelectronic sequence). Conservation of parity in the electrostatic (autoionization) matrix element requires $l_c = l \pm 1$. But the final state of a filled shell (^1S core) plus continuum electron can be $^2l + 1$ and $^2l - 1$ only. Conservation of total L and S in the electrostatic interaction forbids de-

TABLE I. Estimated energy of various $2s\,^1 2p^3(nl)$ levels in Al^{5+}. The entries without (with) parentheses are my estimate (experimental values).

	$Al^{5+} - 1s^2 2s\,^1 2p^4[^4P,^2P]nl$ E (cm^{-1})	
nl	$2s\,^1 2p^4\,^4P(nl)$	$2s\,^1 2p^4\,^2P(nl)$
$3s$	1 195 970 (1 205 000)	1 389 969 (1 359 890)
$3p$	1 267 974	1 461 974
$3d$	1 368 547	1 562 547
$4s$	1 500 946	
$4p$	1 528 419	
$4d$	1 565 460	
$2s^2 2p^3\,^4S$	(1 536 300)	(1 536 300)
∞l	(1 818 300)	(2 012 300)

cay of the ^2L term. Since the radiative decay of the ^2l term is finite the ^2l term should not be included as contributing to the total ionization cross section.

Despite this argument, for neutral Al and sodiumlike Mg, Al, and Si, I assumed unity autoionization yield for the ^2l terms. Earlier[8,9] I had tried to use the forbidden Auger decay of the ^2l term as a basis for a soft x-ray laser scheme in Mg^{1+}. However, inclusion of spin-orbit interaction produces an autoionization rate for the ^2l term substantially larger than the radiative decay rate. I assume this breakdown of LS coupling applies to neutral Al and Al^{2+} and Si^{3+} as well as to Mg^{1+}. A similar conclusion was reached by Griffin *et al.*[10] For the boronlike ions, the LS coupling argument may still be valid as the radiative decay rate is larger.

Cowan and Mann,[6] in their study of Fe^{15+} and Mo^{31+}, have pointed out that $2p^5 3s(nl)^2 l$ terms in the sodium isoelectronic sequence have a zero autoionization rate in LS coupling. Because of the high charge state of these ions it is expected that radiative decay will dominate autoionization arising from spin-orbit mixing. Cowan and Mann[6] further point out that for some excited states radiative decay rates are so large as to dominate the autoionization rate even when the latter is allowed in LS coupling. Cowan and Mann[6] consider the $2p^5 3s 3d$ configuration and show explicitly that for the ^2P and ^2F terms that the autoionization yield is only 0.30 in Fe^{15+} and 0.04 in Mo^{31+}.

For my calculations on Ni^{17+} and Zn^{19+}, I follow Cowan and Mann[6] in excluding the ^2l terms as a contributor to autoionization. Rather than doing explicit calculations on the branching ratio for the $2p^5 3s 3d$ configuration, I use earlier calculations on Auger decay and fluorescence yields.[11] Consider the filled shell $L_{23}M_1M_{4,5}$ Auger transition

$$2p^5 3s^2 3p^6 3d^{10} \rightarrow 2p^6 3s^1 3p^6 3d^9 + ce \ ,$$

where ce stands for continuum electron. If the matrix elements were the same, one finds the Auger rate for $2p^5 3s 3d \rightarrow 2p^6 + ce$ to be $\frac{1}{20}$ of the filled shell rate. Similarly for fluorescence the $2p^5 3s 3d \rightarrow 2p^6 3d$ rate is $\frac{1}{2}$ that for the filled shell case, while the $2p^5 3s 3d \rightarrow 2p^6 3s$ rate is $\frac{1}{10}$ that for the filled shell case. The Auger yield $A_A/(A_A + A_R)$ and radiative yield $A_R/(A_A - A_R)$ are plotted in Fig. 1 as a function of $2p$ ionization energy. To a first approximation, one expects the radiative and Auger decay matrix elements to be approximately constant for the same $2p$ ionization energy. Also shown in Fig. 1 are the autoionization yields of Cowan and Mann[6] for Fe^{15+} and Mo^{31+} at the appropriate $2p$ ionization energies. There is good agreement between the explicit calculations of Cowan and Mann[6] and my simple scaling from Auger rates. Consequently, we used Fig. 1 in treating the autoionization yield of the $2p^5 3s 3d\,^2P$ and ^2F terms in Ni^{17+} and Zn^{19+}.

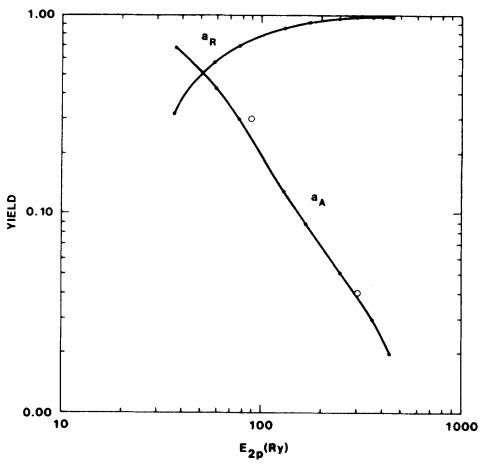

FIG. 1. Auger (a_A) and radiative yield (a_R) for the $2p^5 3s 3d$ configuration as a function of $2p$ ionization energy. Solid lines were obtained using matrix elements for neutral atoms with a $2p$ hole. Circles are calculated values of Ref. 6.

Since these calculations include excitation up to the $5d$ level, a prescription is needed for the higher excitations, e.g., $2p^5 3s 4d$. Without a detailed study of alternative decay modes, e.g., $2p^5 3s 4d \rightarrow 2p^5 3s 3p + h\nu$, etc., any prescription is crude. For these excited levels, I simply excluded ^2l term from the autionization contribution. Relative to excitation of the $2p^5 3s 3l$ levels the higher excitations are weaker and an erroneous treatment of the decay cascade should not produce errors greater than 10% in the total ionization cross section.

III. ELECTRON IONIZATION OF Al IONS

Figure 2 shows the calculated cross sections for Al^{0+}, Al^{1+}, and Al^{2+}. The dashed lines are the direct ionization calculations; the solid line includes also excitation followed by autoionization. The two contributions to the effective ionization cross section are assumed to add directly. The solid points are experimental data. For neutral Al the calculated cross section is significantly higher than the measurements of Shimon *et al.*[4] below 150 eV.

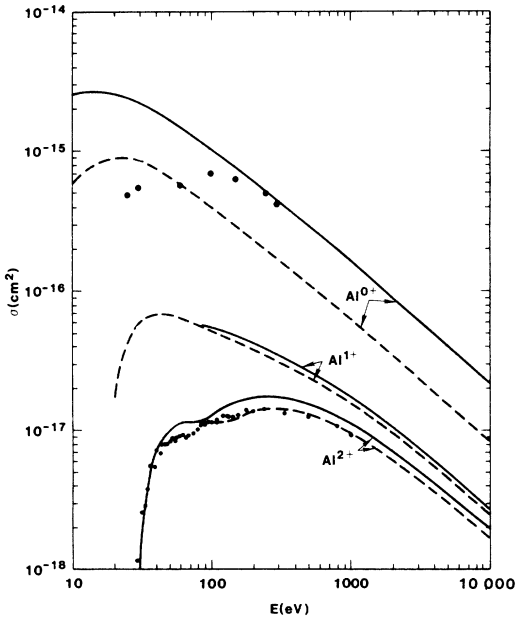

FIG. 2. Calculated direct (dashed curve) and total (solid curve) electron ionization cross section of Al^{0+}, Al^{1+}, and Al^{2+}. Solid points are experimental values for Al^{0+} (Ref. 4) and Al^{2+} (Ref. 5).

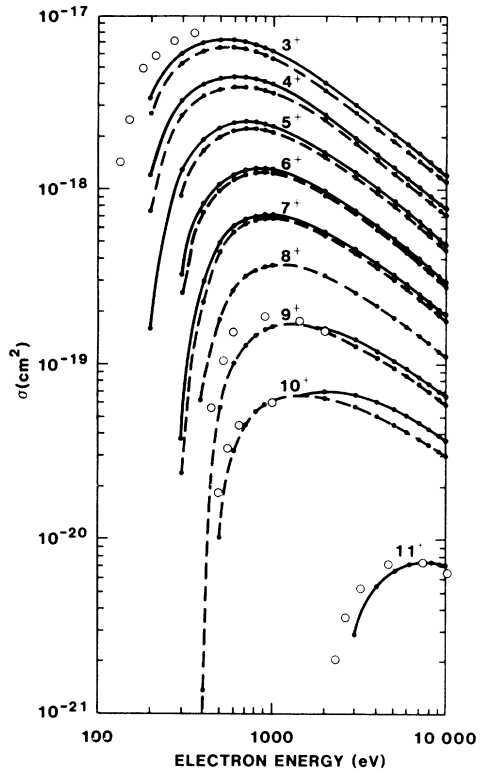

FIG. 3. Calculated direct (dashed curve) and total (solid curve) electron ionization cross section of Al^{n+} $(3 \leq n \leq 11)$. Open circles are distorted-wave ionization calculations of Refs. 12–15.

However, for Al^{2+} the calculations are in reasonable agreement with the measurements of Crandall *et al.*[5] over the whole range of incident energies. This may be fortuitous, particularly near threshold. However, it is surprising that the Al^{2+} calculations agree so much better with experiment below 150 eV while the neutral calculations disagree with experiment. One might ascribe the disagreement in the latter case to the breakdown of the plane-wave Born approximation. This seems unlikely as breakdown of the plane-wave Born approximation should be more severe for Al^{2+} than for the neutral atom.

A more likely explanation lies in the assumption of simple additivity of the cross sections for direct ionization and excitation followed by autoionization. The large cross section for the latter process is due almost entirely to the $3s^2 3p^2 P + e \rightarrow 3s 3p^2\, {}^2L + e$ transition. As discussed in Sec. II, I assume that the ^2L terms all autoionize rapidly compared to radiative decay. After autoionization one has the final state $3s^2 + \epsilon l_c$, where the continuum electron l value (l_c) can be 0 or 2 only. This mode of effective ionization can interfere with the direct process $3s^2 3p + e \rightarrow 3s^2 + \epsilon l_c' + e$, where ($l_c'$) can have any value. A careful treatment of the interference of the processes is beyond the scope of this paper, i.e., it would require treatment of the configuration interaction of $3s3p^2\, {}^2L$ and the $3s^2 ns\, {}^2S$ and $3s^2 nd\, {}^2D$ terms.

In Sec. IV the Al^{2+} cross section is discussed further. In Fig. 3, my calculations for Al^{n+} $(3 \leq n \leq 11)$ are shown. Again the dashed line is direct ionization while the solid line includes excitation followed by autoionization also. For Al^{8+} (boronlike Al) all of the excited terms $1s^2 2s 2pnl$, $n \leq 5$, $l \leq 2$ were estimated to be below the ionization threshold, consequently only a dashed line is shown. Also shown in Fig. 3, as open circles, are interpolations from Younger's distorted-wave ionization calculations for the He,[12] Li,[13] Be,[14] and Ne (Ref. 15) isoelectronic sequences. Characteristically the distorted-wave calculations are higher than the plane-wave Born-approximation calculations near threshold, but there is reasonable agreement at the highest energy in the calculation.

Thus except near threshold there is reasonable agreement between my plane-wave Born-approximation calculations and other calculations and experiments. This indicates that the GOS used

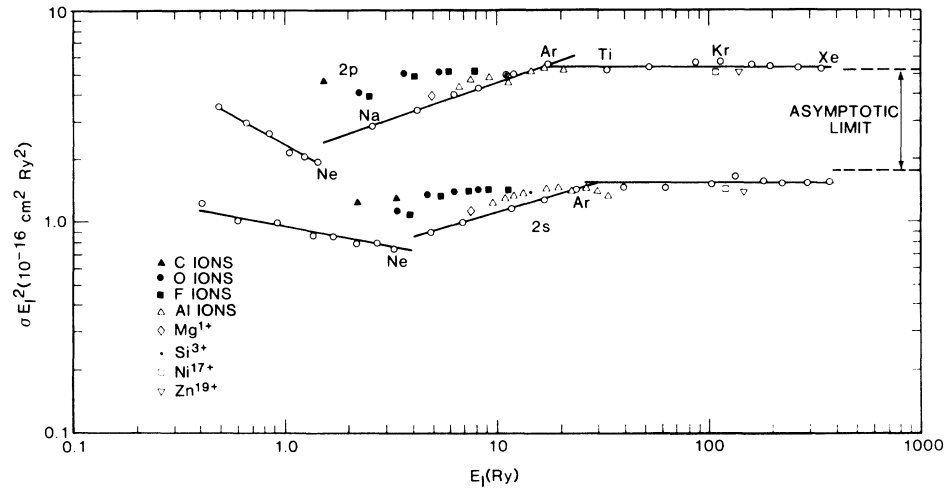

FIG. 4. Peak $2s$ and $2p$ subshell cross sections times subshell ionization energy squared vs ionization energy. Solid lines connect neutral-atom values. Solid points are C, O, and F ion results, while the open points are present calculations for Mg^{1+}, Si^{3+}, Ni^{17+}, Zn^{19+}, and Al ions.

in these calculations should be capable of predicting proton stopping power for the ions to better than 20%.

Finally, in Fig. 4 I compare the scaled neutral-atom $2s$ and $2p$ cross sections[16] with those of Mg^{1+}, Si^{3+}, Ni^{17+}, Zn^{19+}, and the Al ions, adjusted to full shell occupancy. Plotted in Fig. 4 is $\sigma_{\max}E_{nl}^2$ vs E_{nl}. The solid lines connect neutral-atom values, the open points are for these ions, while the solid points are for C, O, and F ions, reported earlier.[3] For the ions treated here the peak cross-section scaling is within 10% of the scaled neutral-atom values.

IV. SODIUM ISOELECTRONIC SEQUENCE

In Fig. 5, I compare my calculated Mg^{1+}, Al^{2+}, and Si^{3+} direct and total cross sections with the recent measurements of Crandall *et al.*[5] For Mg^{1+}, above 20 eV the calculation and the measurements agree to better than 10%. For Al^{2+}, the calculation is as much as 20% higher than the measurements between 40 and 1000 eV. For Si^{3+} the calculation agrees with the measurement to better than 10% above 200 eV and to within 20% below 200 eV. This comparison illustrates the accuracy and applicability over a broad energy range of the plane-wave Born approximation for electron-ion ionization cross sections.

The contribution of excitation followed by autoionization to the total ionization cross section is seen to grow in passing from Mg^{1+} to Si^{3+}, being as much as 30% of the total cross section in the latter case. In Fig. 6, I show the calculated direct and total ionization cross sections for Ni^{17+} and Zn^{19+}, treating autoionization as described in Sec. II. For these ions between 1 and 2 keV, excitation followed by autoionization contributes 65–70% of the total cross section, but the contribution drops to 40% at high incident electron energy. These results are consistent with those of Cowan and Mann[6] for Fe^{15+}.

In Fig. 7 the scaled (by E_{3s}^2) $3s$ subshell cross section for five ions of the Na isoelectronic sequence

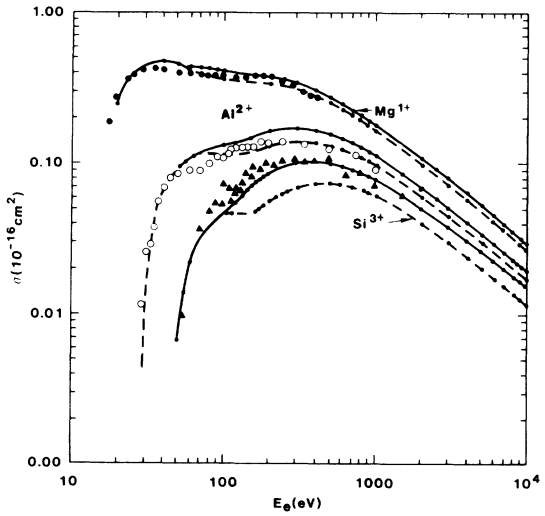

FIG. 5. Calculated direct (dashed curve) and total (solid curve) electron ionization cross section of Mg^{1+}, Al^{2+}, and Si^{3+}. Open and solid points are experimental values from Ref. 5.

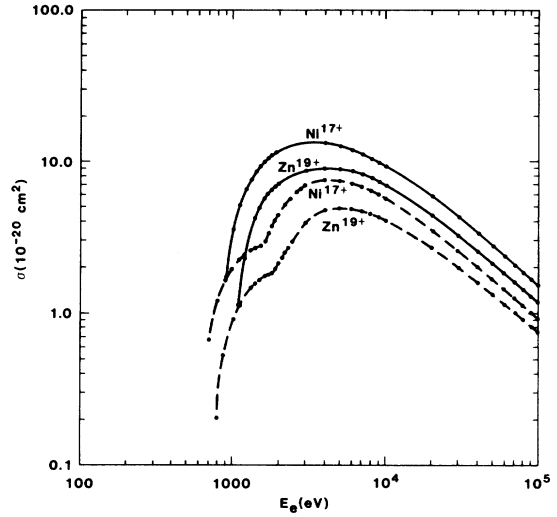

FIG. 6. Calculated direct (dashed curve) and total (solid curve) electron ionization cross section of Ni^{17+} and Zn^{19+}, indicating the relative importance of excitation followed by autoionization.

and for Al^{1+} is compared with values obtained for neutral atoms.[16] The ion data can be fit to better than 5% by the dashed straight line in Fig. 7. Because of the gap in ionization energy between Si^{3+} and Ni^{17+}, these ion calculations are not relevant to the dip seen in the scaled neutral-atom peak 3*s* cross sections.

V. CONCLUSIONS

The Al GOS used in these calculations were generated to calculate proton stopping power for Al ions. The availability of measurements and calculations on electron ionization of Al ions permits a verification of the Al GOS. Except near threshold, as expected, my calculated Al-ion cross sections agree with the measurements and other calculations to 20%. This provides some confidence that the Al stopping-power calculations are at least that accurate.

A comparison of the calculation with measurements on neutral Al and Al^{2+} strongly suggests that for neutral Al the processes of direct ionization and excitation followed by autoionization are not simply additive.

For the Na isoelectronic sequence, the calculations are in excellent agreement with recent measurements in Mg^{1+}, and in good agreement with the measurements in Al^{2+} and Si^{3+}. For Ni^{17+} and Zn^{19+} we find that excitation followed by autoionization contributes 65% of the total ionization cross section at low incident electron energy and 40% at high energy, in agreement with recent calculations in Fe^{15+}.

In comparing scaled subshell cross-section maxi-

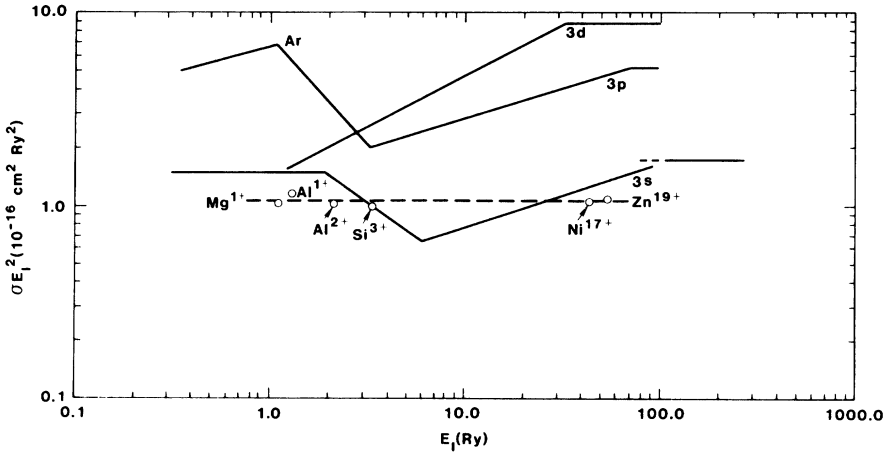

FIG. 7. Peak electron ionization cross section times subshell ionization energy squared for the 3*s*, 3*p*, and 3*d* subshells. Solid lines connect neutral-atom values. Open circles are 3*s* subshell values (adjusted to two 3*s* electrons) from the calculations on the Na isoelectronic sequence and Al^{1+}. Dashed line is a possible alternative scaling for ions.

ma ($\sigma_{max}E_{nl}^2$) with results for neutral-atom results, better agreement is found for the ions studied here than for ions of C, O, and F. The results of this and an earlier paper suggest that the plane-wave Born approximation is an excellent tool for calculating electron-ion ionization cross sections, except near threshold.

ACKNOWLEDGMENTS

I wish to thank Dr. D. H. Crandall of ORNL for providing an unpublished manuscript of his group's work (Ref. 5) and of the work of Griffin *et al.* (Ref. 10). This work was supported by the U. S. Department of Energy.

[1]E. J. McGuire, J. M. Peek, and L. C. Pitchford (unpublished).

[2]H. A. Bethe, Ann. Phys. (Leipzig) 5, 325 (1930); Z. Phys. 76, 293 (1932).

[3]E. J. McGuire, Phys. Rev. A 25, 192 (1982).

[4]L. L. Shimon, E. I. Nepiipov, and I. P. Zapescochnyi, Zh. Tekh. Fiz. 45, 688 (1975). [Sov. Phys.—Tech. Phys. 20, 434 (1975)].

[5]D. H. Crandall, R. A. Phaneuf, R. A. Falk, D. S. Belic, and G. H. Dunn, Phys. Rev. A 25, 143 (1982).

[6]R. D. Cowan and J. B. Mann, Astrophys. J. 232, 940 (1979).

[7]C. E. Moore, *Atomic Energy Levels,* National Standard Reference Data Service (National Bureau of Standards, Washington, D.C., 1971), Vol. 1, Circ. No. 35. A recent, more extensive, tabulation of levels for Al ions [W. C. Martin and R. Zalubas, J. Phys. Chem. Ref. Data 8, 817 (1979)] does not contain additional levels of the form $2s^12p^m(n\bar{l})$.

[8]E. J. McGuire, Phys. Rev. A 14, 1402 (1976).

[9]E. J. McGuire and M. A. Duguay, Appl. Opt. 16, 83 (1977).

[10]D. C. Griffin, C. Bottcher, and M. Pindzola, Phys. Rev. A 25, 154 (1982).

[11]E. J. McGuire, Phys. Rev. A 3, 587 (1971), and Sandia Research Report No. SC-RR-710075 (unpublished).

[12]S. M. Younger, Phys. Rev. A 22, 1425 (1980).

[13]S. M. Younger, Phys. Rev. A 22, 111 (1980).

[14]S. M. Younger, Phys. Rev. A 24, 1278 (1981).

[15]S. M. Younger, Phys. Rev. A 23, 1138 (1981).

[16]E. J. McGuire, Phys. Rev. A 16, 73 (1977).